Supporting Information

Graphene Oxide Membranes with Narrow Inter-Sheet Galleries for Enhanced Hydrogen Separation

Amr F. M. Ibrahim[a,b], Fateme Banihashemi[b], Y.S. Lin[b],*

[a] Faculty of Petroleum and Mining Engineering,
Suez University, Suez, Egypt.
[b] School for Engineering of Matter, Transport and Energy
Arizona State University, Tempe, AZ 85287-6006, USA.

Experimental

GO powder used in this work is prepared by a modified version of Brodie's method [1]. 10 ml of fuming nitric acid was charged into a flask equipped with a Teflon mechanical stirrer. The flask was cooled down to 0 °C using an ice bath. 1g graphite flakes (Sigma-Aldrich, SKU: 332461, ~150 μm flakes) was added to the flask under stirring. 5 min later 10 g potassium chlorate (KClO$_3$, Alfa Aesar, +99.0%), was slowly added in small doses to the mixture under stirring in a period of 30 min. The whole mixture was then stirred for 30 min, then the obtained dark green thick slurry was left unstirred at ambient temperature for 24 h. The loss of nitric acid due to evaporation was retrieved by adding another 10 ml of nitric acid. The slurry was then heated to 60 °C using a tab water bath and kept at this temperature for 8 h while stirring. The reaction was terminated by transferring the pasty mixture into 500 ml of distilled water.

Homemade vacuum filtration system was used to deposit 30 ml (0.006 mg/ml) GO suspension on hydrophilic macroporous polyester track etch substrates (pore diameter of 0.1μm) obtained from commercial resources (Sterlitech, SKU: PET0125100). The produced GO membranes were dried at room temperature under vacuum for 24 h before characterization and permeation tests.

GO nanosheets and membranes were characterized by XRD for phase structure and crystallinity (Bruker D8 ADVANCE X-ray diffractometer; Cu Kα radiation λ= 1.542 Å at 40 kV and 40 mA, scan step of 0.05°). Scanning electron microscope (SEM, Amray 1910) was used for imaging membrane surface topology and cross-section as well as the lateral dimension of GO sheets. Fourier transform infrared (FT-IR, Thermo Nicolet 6700) was used to identify surface functional groups of GO nanosheets. Raman spectroscopy measurements were performed on a Renishaw InVia Raman microscope with a 488-nm laser for excitation to quantify defects of GO powder.

Gas permeation experiments of the prepared GO membranes were conducted on a multicomponent gas permeation/separation system [2]. A PETE supported GO membrane was mounted in a stainless-steel membrane cell, with the GO layer facing the feed side, and sealed by silicone O-rings, where the permeation area is 3.14×10^{-4} m^2. Pure gases and gas mixture experiments were performed in the Wicke Kallenbach configuration with atmospheric feed at room temperature and zero transmembrane pressure difference to compare permeation results to the works done in literature. The total flow rate at the feed side was controlled using mass flow controllers at 25 ml/min for single gas experiments and at 50 ml/min in 50/50 vol.% binary (H_2/CO_2) gas mixtures. The permeate side was swepted by 25 ml/min argon. Gas permeation data is reported as a mean of three measurements and a maximum error of 5%. Compositional analysis of permeate and retentate streams was determined using gas chromatography (Agilent Technologies, 6890 N). The reproducibility of the synthesis method was as high as 90% after investigating of prepared GO membranes performance.

GO-B   GO-H
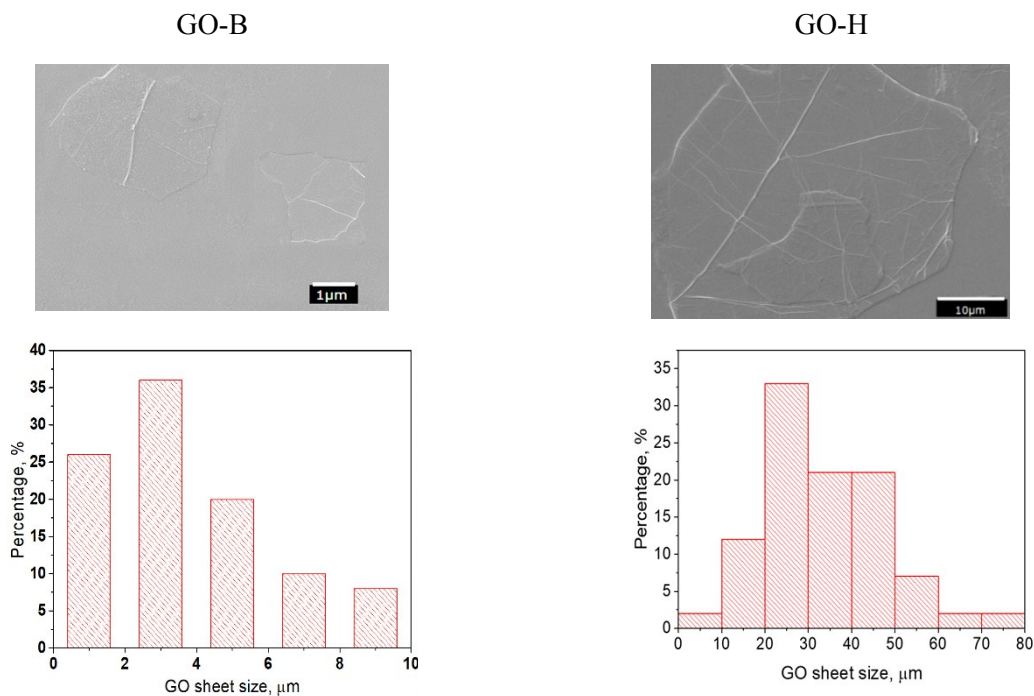
Fig. S1 SEM images and corresponding histograms of GO-B sheets produced in this work using Brodie's method compared to GO-H sheets produced using Hummers' method from our previous publication.[2]

The corresponding histograms for the sheet size distributions were obtained by measuring the longest lateral dimension of 100 sheets in GO-B and GO-H samples and the average size of GO-B and GO-H sheets is about 3.5 and 30 μm respectively.
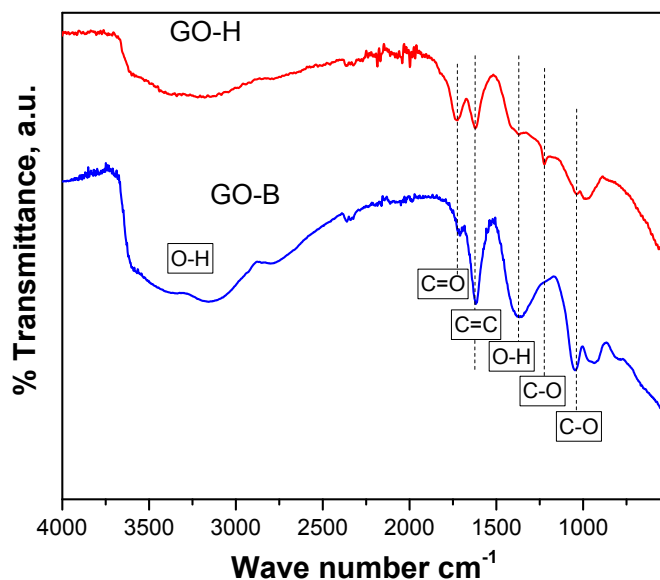
Fig. S2 FT-IR spectra of GO powder produced using Brodie's method compared with GO sample produced using Hummers' method [1]

The FTIR spectrum for GO-B and GO-H are very similar in general exhibiting the same peaks, however, the relative intensity of some peaks is remarkably different, which shows that Hummers' and Brodie's synthesis methods indeed result in different chemical functionalities of GO. The spectrum exhibits overlapping bands in the 3650 cm^{-1} to 3000 cm^{-1} range which indicates the presence of hydroxyl groups (O-H stretching vibration of free hydroxyl groups of physiosorbed water and C-OH, stretching vibration of structural hydroxyl groups of GO). No clear distinction seems possible between C-OH and H$_2$O peaks. [3, 4] However, The GO-B sample has stronger spectral features for 3650 cm^{-1} to 3000 cm^{-1} range and also for the adsorption band at 1369 cm^{-1} assigned for (C–OH) bending vibrations. [5] On the other hand, the GO-B powder shows less pronounced signals from the (C=O) stretching vibration assigned to carboxyl groups at1725 cm^{-1} and (C-O) epoxy stretching vibration at 1222 cm^{-1}. [5] Other prominent signals in the GO's spectrum such as those at 1620 cm^{-1} and 1036 cm^{-1} originate from the stretching of unoxidized graphitic sp^2 (C=C) and the (C-O) alkoxy stretching, respectively. [6]

4
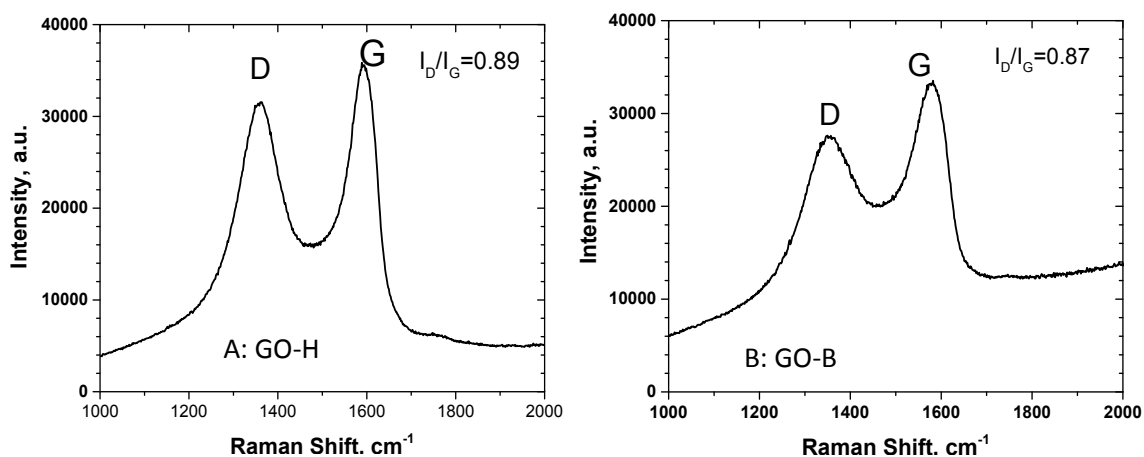
Fig. S3 Raman spectra of GO powder samples prepared by: (A) Hummers' and (B) Brodie's methods.

The G and D bands for GO-B and GO-H samples were noticed at 1584 and 1590 cm^{-1} and 1348 and 1355 cm^{-1} respectively. Cançado and coworkers [7] developed a methodology to correlate the (I_D/I_G) ratio with the distance between point-like defects (L_D) and defect density, n_D on single layer graphene. This dependence of (I_D/I_G) on L_D was also applied to GO and chemically reduced GO. [8] According to Cançado, [7] it is possible to distinguish between stage 2 ($L_D < 3$ nm) and stage 1 ($L_D > 10$ nm) by analyzing Raman spectra in terms of full width at half maximum (FWHM). For stage 1 a FWHM of about 20 and 14 cm^{-1} would be expected for D and G peaks respectively [7]. The FWHM of the D and G peaks are 140 and 163 cm^{-1} for GO-B and 196 and 108 cm^{-1} for GO-H respectively, and thus typical of stage 2 region. Based on equations 1 and [7, 9] with excitation energy, $E_L = 2.54$ eV for the used He-Ne (488-nm) laser, L_D is about 1.39 and 1.4 nm and the defect density (n_D µm^{-2}) is 162780 and 159122 for GO-B and GO-H respectively.

$$L_D^2(nm^2) = 5.4 \times 10^{-2} E_L^4 \tag{1}$$

$$n_D(\mu m^{-2}) = 10^8 / \pi L_D^2 \tag{2}$$
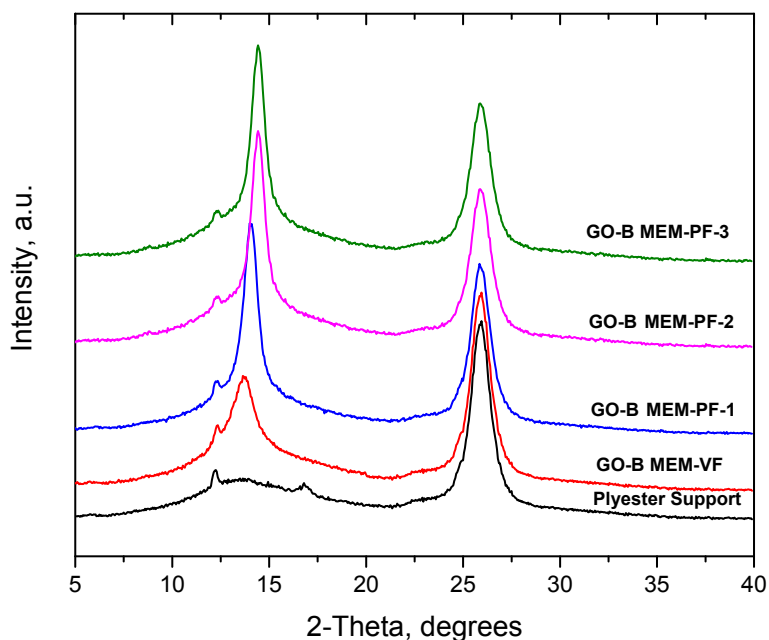
Fig. S4 XRD patterns of GO-B membranes on polyester substrate prepared by vacuum (VF) and pressurized (PF) filtration at pressures of 1, 2, 3 bar.

XRD patterns in Figure S4 show that the GO peak of GO-B MEM-VF made by vacuum filtration is broader and less intense compared to the GO peak for GOB-MEM-PF-1 made by pressurized filtration, which suggest better stacking of the GO sheets in pressurized filtration system. The reduction in the rate of applied vacuum due to the growth of the GO film during vacuum filtration may cause the sheets far from the support surface to be loosely packed and less ordered compared to the sheets directly on the support surface. The GO peak shifts to a larger angle when pressure is applied in the filtration system and a further shift is noticed when the pressure increases from 1 to 3 bar. These results indicate an enhancement of the packing and stacking density of GO-B sheets as a function of applied filtration pressure.
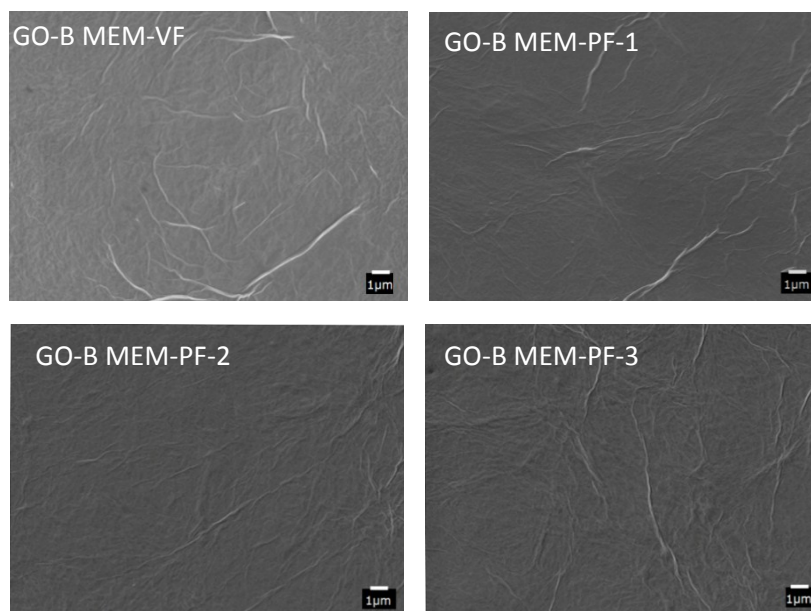
Fig. S5 SEM surface images of GO membranes prepared by vacuum and pressure filtration using GO-B.

The SEM images of the surface and cross sections of the synthesized GO-B membranes using vacuum and pressure filtration are given in Fig.S5. Overall, the surface is relatively corrugated, showing sheet edges and extrinsic wrinkles with no obvious defects (pores or cracks). The surface height of wrinkles was also noticed to decrease with increasing the applied pressure in pressurized filtration system.
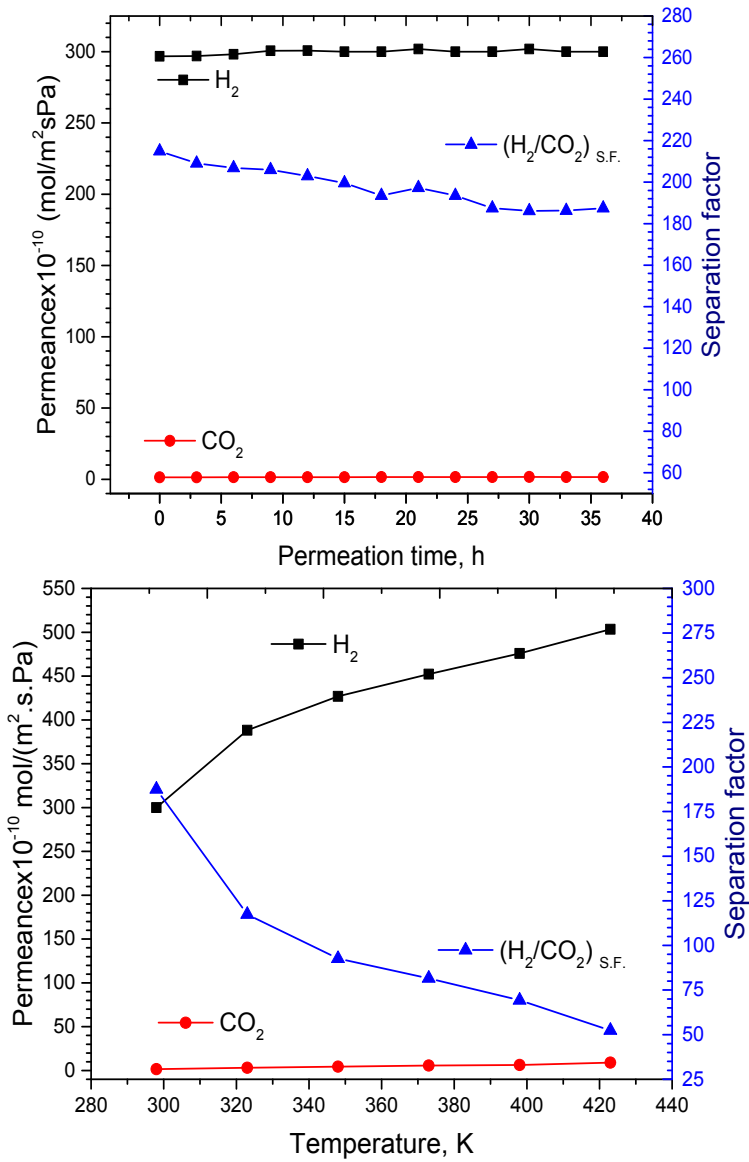
Fig. S6. H_2/CO_2 equimolar mixture separation performance of GO-B membranes prepared in this work by pressurized filtration (PF) at pressures of 2 bar as a function of: [A] permeation time and [B] temperature.

Table S1 Comparison of ideal selectivity and binary separation factor of H_2/CO_2 at room temperature for GO-B membranes synthesized in this work by pressure filtration.

Membrane	Interlayer spacing, Å	Ideal pure gas data			Binary mixture data		
		Permeance 10^{-8} mol/(m^2.s.Pa)		Ideal H_2/CO_2 selectivity	Permeance 10^{-8} mol/(m^2.s.Pa)		Mixture H_2/CO_2 separation factor
		H_2	CO_2		H_2	CO_2	
MEM-PF-1	3.1	3.77	0.025	168.4	3.15	0.033	100.1
MEM-PF-2	3.0	3.53	0.007	504.3	2.90	0.010	214.2
MEM-PF-3	3.0	3.65	0.008	457.5	2.93	0.012	190.4

Among the GO-B membranes synthesized in this work, the membranes made using pressurized filtration system show more reduction in the permeability of large gas molecules compared to those made using vacuum filtration and thus more improved H_2/CO_2 selectivity. The packing density might be expected to increase as the filtration pressure increases; however, higher pressures lead to a faster filtration process, and this may lead to defects in the GO film.

References

1   B. C. Brodie, Philos. Trans. R. Soc. of London, 1859, 1**49**, 249-259.
2   A. Ibrahim and Y. S. Lin, *J. Membr. Sci.*, 2018, **550**, 238-245.
3   T. Szabó, O. Berkesi, P. Forgó, K. Josepovits, Y. Sanakis, D. Petridis and I. Dékány, *Chem.Mater.*, 2006, **18**, 2740-2749.
4   S. Cerveny, F. Barroso-Bujans, Á. Alegría and J. Colmenero, *J. Phys. Chem. C*, 2010, **114**, 2604-2612.
5   S. You, S. M. Luzan, T. Szabó and A. V. Talyzin, *Carbon*, 2013, **52**, 171-180.
6   J. Zhang, H. Yang, G. Shen, P. Cheng, J. Zhang and S. Guo, *Chem. Commun.*, 2010, **46**, 1112-1114.
7   L. G. Cançado, A. Jorio, E. H. M. Ferreira, F. Stavale, C. A. Achete, R. B. Capaz, M. V. O. Moutinho, A. Lombardo, T. S. Kulmala and A. C. Ferrari, *Nano Lett.*, 2011, **11**, 3190-3196.
8   S. Eigler, C. Dotzer and A. Hirsch, *Carbon*, 2012, **50**, 3666-3673.
9   A. C. Ferrari and J. Robertson, *Phys. Rev. B*, 2000, **61**, 14095-14107.
10 L. M. Robeson, *J. Membr. Sci.*, 2008, **320**, 390-400.